

# Delocalization and hybridization enhance the magnetocaloric effect in Cu-doped Ni<sub>2</sub>MnGa

S. Roy,<sup>1</sup> E. Blackburn,<sup>2</sup> S. M. Valvidares,<sup>3</sup> M. R. Fitzsimmons,<sup>4</sup> S. C. Vogel,<sup>4</sup> M. Khan,<sup>5</sup> I. Dubenko,<sup>5</sup> S. Stadler,<sup>5</sup> N. Ali,<sup>5</sup> S. K. Sinha,<sup>6</sup> and J. B. Kortright<sup>3</sup>

<sup>1</sup>*Advanced Light Source, Lawrence Berkeley National Laboratory, Berkeley, California 94720, USA*

<sup>2</sup>*School of Physics and Astronomy, University of Birmingham, Birmingham, B15 2TT, United Kingdom*

<sup>3</sup>*Materials Sciences Division, Lawrence Berkeley National Laboratory, Berkeley, California 94720, USA*

<sup>4</sup>*Manuel Lujan Neutron Scattering Center, Los Alamos National Laboratory, Los Alamos, New Mexico 87545, USA*

<sup>5</sup>*Department of Physics, Southern Illinois University, Carbondale, Illinois 62901, USA*

<sup>6</sup>*Department of Physics, University of California, San Diego, La Jolla, California 92093, USA*

(Received 8 January 2009; revised manuscript received 1 June 2009; published 22 June 2009)

The structural and magnetic transitions in the shape-memory alloy Ni<sub>2</sub>MnGa can be tuned as a function of temperature by adding dopants. By altering the free energy such that the structural and magnetic transitions coincide, a giant magnetocaloric effect is created near room temperature. We show, using x-ray absorption spectroscopy and x-ray magnetic circular dichroism, how Cu, substituted for Mn, pulls the magnetic transition downward in temperature and also, counterintuitively, increases the delocalization of the Mn magnetism. At the same time, this reinforces the Ni-Ga chemical bond, raising the temperature of the martensite-austenite transition. At 25% doping, the two transitions coincide at 317 K.

DOI: [10.1103/PhysRevB.79.235127](https://doi.org/10.1103/PhysRevB.79.235127)

PACS number(s): 75.30.Sg, 61.05.F–, 71.20.Lp, 81.30.Kf

## I. INTRODUCTION

The Heusler alloys of the type Ni-Mn-X, where X=Ga, In, Sb, and Sn, combine a first-order structural-phase transition (cubic to tetragonal) with magnetic transitions in both structural phases. By doping, or by altering relative concentrations, these transitions can be shifted, giving rise to a wide array of different functionalities, for example, shape-memory effects and giant magnetoresistance.<sup>1–4</sup>

In this paper, we concentrate on the Ni-Mn-Ga alloys, which have previously been studied as examples of shape-memory materials. In the parent compound, Ni<sub>2</sub>MnGa, the magnetostructural transition occurs at 225 K and there is a second-order transition from paramagnetism to ferromagnetism at 384 K.<sup>5</sup> The magnetostructural phase transition is associated with a magnetocaloric effect, that is, a change in temperature due to a variation in external magnetic field.<sup>6,7</sup>

When the structural and magnetic transitions are tuned to occur at the same temperature, the magnetic part of the entropy change (a measure of the magnetocaloric effect) of the joint transition is significantly enhanced relative to that of the separate transitions. For example, by increasing the Ni content, entropy changes in the range of –3.5 to –20.4 J/kg K have been obtained in polycrystals while in single crystals the change observed has been as high as –86 J/kg K.<sup>1,3,8</sup> The transitions can also be tuned by atomic substitution at the Mn or the Ga sites.<sup>5,9</sup> In particular, 25% Cu at the Mn site results in a  $\Delta S$  of –60 J/kg K in the temperature range of 308–334 K.<sup>10,11</sup>

On the basis of this, the Ni-Mn-Ga alloys have been classified as giant magnetocaloric (GMC) compounds. Other examples of GMC compounds include Gd<sub>5</sub>(SiGe)<sub>4</sub>,<sup>12</sup> and MnFeP<sub>1–x</sub>As<sub>x</sub>.<sup>13</sup> These materials have been suggested for use in solid-state cooling technology, with obvious advantages for small scale local cooling and the potential to eventually replace existing gas-based refrigeration technologies that use chloro-fluoro- and hydro-fluoro-carbon chemicals known to

have a severe detrimental effect on human health and the environment.<sup>14</sup>

Ni<sub>2</sub>Mn<sub>0.75</sub>Cu<sub>0.25</sub>Ga (NMCG) is therefore a promising magnetic refrigerant. However, the physics governing the shift of the transition temperatures and the role of dopants, namely, the origin behind the increased entropy, has not been convincingly elucidated. This paper provides a systematic experimental study of the electronic structure in Ni<sub>2</sub>MnGa and NMCG to address this issue.

Ferromagnetism in the Ni<sub>2</sub>MnGa family of compounds is localized and is primarily due to indirect Ruderman-Kittel-Kasuya-Yoshida interactions between neighboring Mn atoms mediated by conduction electrons.<sup>15,16</sup> The Mn minority-spin *d* electrons are almost excluded from the conduction band and hence give rise to a localized magnetic moment. Since the magnetic and structural properties are intricately linked by the lattice-parameter ratio *c/a* (Refs. 17–20) as well as the density of the 3*d* electrons at the Fermi level,<sup>20,21</sup> replacement of Mn by Cu should cause site- and element-specific changes in the electronic and magnetic properties.

We have performed systematic x-ray absorption spectroscopy (XAS) and x-ray magnetic circular dichroism (XMCD) measurements at the *L*<sub>2,3</sub> edges of the constituent elements of Ni<sub>2</sub>MnGa and NMCG as a function of temperature to directly probe the *d* electrons and their respective contributions to the electronic and magnetic properties. Magnetization and the nature of the phase transition have been determined by magnetometry and neutron-diffraction studies. We find that Cu substitution has two main effects. First, it increases the covalent character of Ni, resulting in an enhanced Ni-Ga hybridization that affects the martensitic transition temperature. Second, reducing the Mn concentration reduces the magnetic ordering temperature and makes the system more delocalized from the magnetism point of view. The combined XAS, XMCD, neutron, and magnetometry results lead to a coherent atomic-scale understanding of how alloying-induced changes in the electronic properties lead to the en-

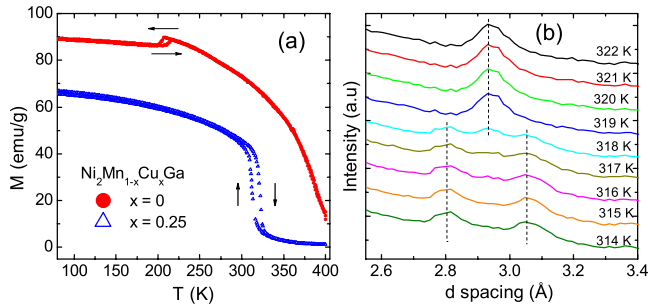


FIG. 1. (Color online) (a) Magnetization vs temperature curves for  $\text{Ni}_2\text{MnGa}$  (closed red circles) and  $\text{Ni}_2\text{Mn}_{0.75}\text{Cu}_{0.25}\text{Ga}$  (open blue triangles) for both increasing and decreasing temperatures measured in an external field of 1 kOe. (b) Neutron diffraction tracking the cubic (002) Bragg peak as a function of temperature for  $\text{Ni}_2\text{Mn}_{0.75}\text{Cu}_{0.25}\text{Ga}$ , showing the coexistence of cubic ( $a = 5.814 \text{ \AA}$ ) and tetragonal phases during the magnetostructural phase transition. Vertical dashed lines are guides to the eye to show peak positions.

hanced thermodynamics properties of the giant magnetocaloric effect in NMCG.

## II. EXPERIMENTAL METHODS

Polycrystalline stoichiometric ingots of  $\text{Ni}_2\text{MnGa}$  and NMCG were made from high-purity elemental Ni, Mn, Cu, and Ga using the conventional arc-melting technique. Details of sample preparation can be found elsewhere.<sup>5,9–11</sup> The phase purity of the samples was checked by x-ray diffraction using  $\text{Cu } K_\alpha$  radiation at room temperature. Magnetization measurements were carried out using a superconducting quantum interference device (SQUID) magnetometer (Quantum Design, Inc.). Neutron diffraction was carried out on powdered samples at the Asterix (polarized neutrons) and the high pressure preferred orientation (HIPPO) (unpolarized neutrons) beamlines at the Manuel Lujan Neutron Scattering Center, Los Alamos National Laboratory. XAS and XMCD spectra were measured at beamline 4.0.2 of the Advanced Light Source, Lawrence Berkeley National Laboratory. A small slice of the sample was cut from the bulk immediately prior to measurement to avoid surface contamination. Circularly polarized x rays tuned to the  $L_{2,3}$  edges of Ni, Mn, Cu, and Ga were incident normal to the sample surface. The absorption was measured by the total electron-yield method. The measurements were carried out at temperatures of 80, 300, and 330 K at an applied magnetic field of 1 T.

## III. RESULTS

### A. Magnetostructural transition

Figure 1(a) shows the magnetization versus temperature curves from 75 to 400 K for  $\text{Ni}_2\text{MnGa}$  and NMCG taken at 1 kOe.  $\text{Ni}_2\text{MnGa}$  shows a second-order paramagnetic-to-ferromagnetic phase transition at 386 K ( $T_C$ ) and a first-order change in magnetization at 208 K ( $T_M$ ) associated with the martensitic structural transition. On substituting Mn by Cu the second-order magnetic and first-order structural transi-

tion temperatures move toward each other, and for 25% Cu merge into a single first-order phase transition at 317 K [Fig. 1(a)].<sup>10</sup> This merging of  $T_C$  and  $T_M$  comes at the cost of an overall reduction of magnetization in NMCG as compared to  $\text{Ni}_2\text{MnGa}$ . This reduction is  $\sim 25\%$  and correlates with the decreased Mn concentration. The nature of the phase transition has been further confirmed by temperature-dependent neutron diffraction [Fig. 1(b)]. The single (002) peak above the transition temperature splits due to the cubic-tetragonal structural transition. The presence of three clear peaks around the phase-transition temperature ( $315 \text{ K} \leq 318 \text{ K}$ ) shows that the cubic austenitic and tetragonal martensitic phases coexist close to the transition. This confirms the first-order nature of the magnetostructural transition in NMCG. The first-order nature of the magnetostructural transition complicates the thermodynamic interpretation of the thermomagnetization data in terms of the magnetocaloric effect and thus care should be taken in determining its magnitude.<sup>22,23</sup>

### B. $\text{Ni}_2\text{Mn}_{0.75}\text{Cu}_{0.25}\text{Ga}$ : changes with temperature

To understand the underlying effects of Cu substitution, we first determine the changes in electronic and magnetic structures in NMCG due to the phase transition, and then compare the properties of NMCG with the parent compound  $\text{Ni}_2\text{MnGa}$ . Changes in the electronic structure of the constituent elements of NMCG were determined from XAS measured at 80 and 300 K [Figs. 2(a)–2(d)]. The multiplet structure evident at the Ni and Mn  $L_{2,3}$  edges in these metallic samples is taken to result from partial localization of the  $3d$  states induced by the core hole of the excited atom and from hybridization effects reflecting the ground-state band structure. For Ni, multiplet structures at the  $L_3$  are the features marked as A and B, and, although weak, are clearly present at the  $L_2$  edge (feature C). There is no significant change in A over the entire temperature range measured while feature B weakens and shifts upward in energy on lowering the temperature [by 1.5 eV at 80 K relative to 300 K—see inset of Fig. 2(a)]. This feature B, which is 5 eV above the main  $L_3$  peak, represents the Ni  $2p3d^{10}$  state that hybridizes with the Ga  $p$  states.<sup>24</sup> Extending this interpretation, we thus interpret the broadening of feature B due to the martensitic transition as evidence of an increase in the covalent character of Ni resulting from increased hybridization with Ga. A similar shift is also observed for feature C in Fig. 2(a).

The Mn XAS [Fig. 2(b)] also shows multiplet structure (features D–F) characteristic of primarily  $d^5$  with some  $d^6$  ground states. Although there are discussions about selective oxidation in the literature as the reason for the multiplet features in the Mn, experimental results reported on similar compounds increasingly suggest that a modification of the band structure is responsible for the observed line shapes.<sup>24–27</sup> This is consistent with band-structure calculations,<sup>16,20,28</sup> and the observation of the Jahn-Teller effect in these compounds, which lifts the  $d$ -orbital degeneracy and effectively narrows the band.<sup>29</sup>

A weak bump (feature F) is observed 5 eV above the main peak (637.4 eV)—inset of Fig. 2(b). The integrated intensity

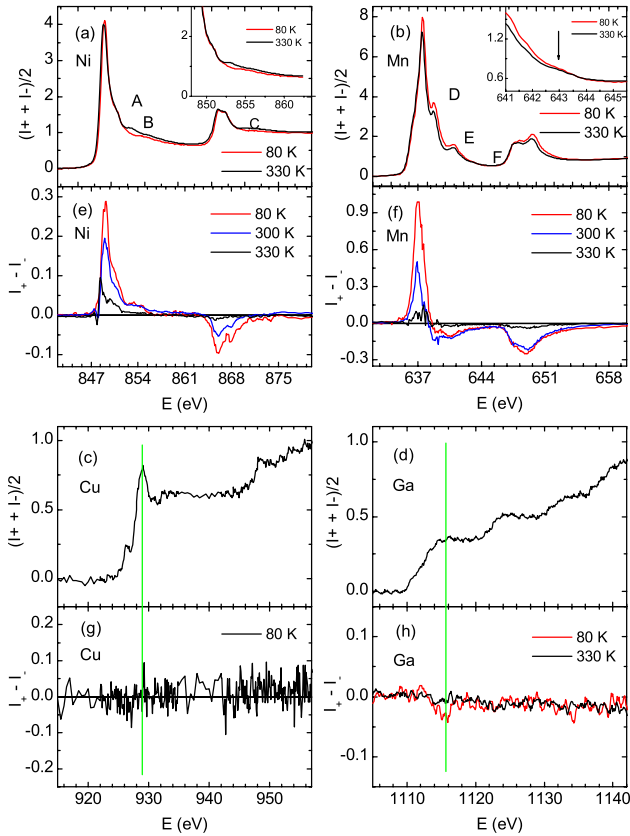


FIG. 2. (Color online) XAS curves at the (a) Ni, (b) Mn, (c) Cu, and (d) Ga  $L$  edges for  $\text{Ni}_2\text{Mn}_{0.75}\text{Cu}_{0.25}\text{Ga}$  at 80 (red line) and 330 K (black line). The XMCD curves at  $T=80, 300,$  and  $330$  K are in (e)–(h), respectively. The inset in (a) shows the Ni XAS around the peak marked B while the arrow in the inset of (b) shows the Mn XAS around the feature marked F. Green lines in (c) and (d), and (g) and (h) are guides to the eye to show the absence (presence) of XMCD at the  $L_3$  peak of Cu (Ga), respectively.

under this feature (Gaussian fit) reveals that the peak is stronger at 330 K by  $\sim 9\%$  than at 80 K with no change in peak position while the corresponding peak in  $\text{Ni}_2\text{MnGa}$  at 80 K is  $\sim 25\%$  stronger. Similar peaks, previously observed in Heusler alloys and Mn-based oxide systems, have been interpreted as due to  $d$ - $d$  and/or charge transfer causing a redistribution of the  $3d$  electrons.<sup>25,30</sup> While we do not attempt to distinguish between these two possible origins of this feature, the change in its intensity with temperature shows that the magnetostructural transition as well as Cu doping results in a redistribution of the  $d$  electrons. Furthermore, since the peak is weaker for NMCG than for  $\text{Ni}_2\text{MnGa}$ , it shows that the itinerancy of the  $3d$  electrons is larger than in the parent compound. The Cu and Ga XAS show no discernible changes as a function of temperature.

XMCD spectra taken at 80, 300, and 330 K are shown in Figs. 2(e)–2(h). Both Ni and Mn XMCD show multiplet structure at the  $L_{2,3}$  edges consistent with published results.<sup>24,25,31</sup> In the ferromagnetically ordered state the Mn atomic moment increases by 61% at 80 K relative to 300 K. In comparison, the Ni moment only changes by 33%. The smaller change in the Ni moment relative to Mn is attributed to minority-spin antibonding states above  $E_F$  which are pri-

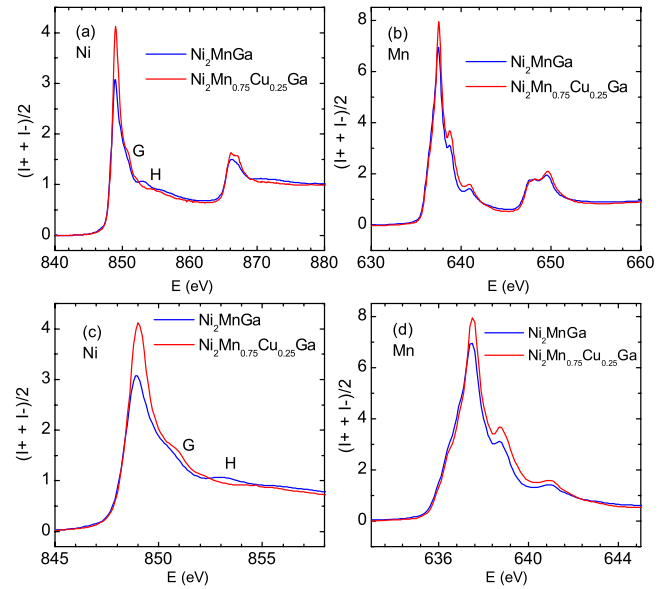


FIG. 3. (Color online) XAS curves at the (a) Ni and (b) Mn  $L$  edges for  $\text{Ni}_2\text{MnGa}$  (blue line) and  $\text{Ni}_2\text{Mn}_{0.75}\text{Cu}_{0.25}\text{Ga}$  (red line) at 80 K. For clarity the XAS at the  $L_3$  edge alone for Ni and Mn is replotted in (c) and (d), respectively.

marily due to Mn while both the  $e_g$  states of Ni are below  $E_F$ .<sup>20</sup>

A significant dichroic signal was detected at the Ga  $L_3$  edge and it follows the same temperature dependence as the Ni (Mn) magnetization by disappearing above  $T_C$ . The Ga-XMCD signal is opposite to that of Ni and Mn which means that Ga induced spins are antiparallel to Ni and Mn spins, in accord with published results.<sup>16,29</sup> Recalling our earlier result from Fig. 2(a) that for  $T < T_M(T_C)$  the covalent character of Ni increases, the magnetic moment in Ga is then due to hybridization effects between Ni  $d$  states and Ga  $p$  states, and does not come from direct-exchange interactions. It is interesting to note that similar hybridization effects between Gd and Ge are also found in  $\text{Gd}_5(\text{SiGe})_4$  compounds.<sup>32</sup> Within the noise level, we did not observe any magnetic moment for Cu.

### C. $\text{Ni}_2\text{Mn}_{0.75}\text{Cu}_{0.25}\text{Ga}$ : comparison with $\text{Ni}_2\text{MnGa}$

The effect of Cu substitution on the electronic structure in Ni and Mn is obtained from XAS measured at 80 K [Figs. 3(a)–3(d)]. Significant change on Cu substitution is seen at the feature H, which is the same feature as B in Fig. 2(a). This feature is a distinct bump in  $\text{Ni}_2\text{MnGa}$ , whereas it is broadened in NMCG [see Fig. 2(a)] and moved to higher energy. Mn XAS does not show a qualitative change in spectral shape [Figs. 3(b) and 3(d)]. Changes are also observed in the intensity where both the Ni and Mn XAS have systematically higher intensity for NMCG than  $\text{Ni}_2\text{MnGa}$  implying that there are fewer filled  $d$  states immediately around Ni and Mn in NMCG. This is indicative of a “ground-state” transfer of charge away from Ni and Mn. Given the slightly higher electronegativity of Cu as compared with Mn or Ni, it is possible that Cu takes charge away from the Ni and Mn sites

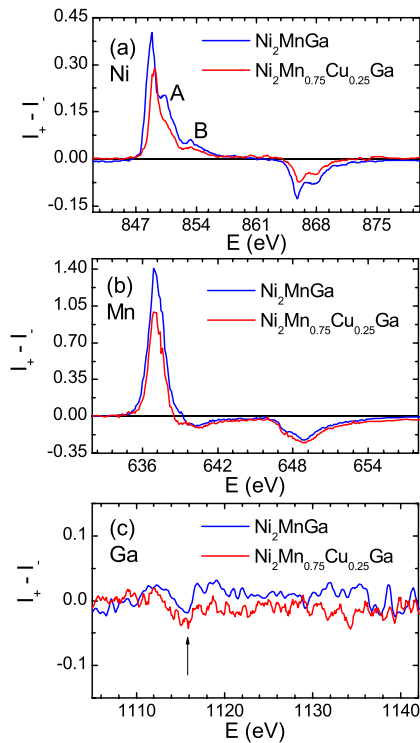


FIG. 4. (Color online) [(a)–(c)] XMCD curves for Ni, Mn, and Ga for  $\text{Ni}_2\text{MnGa}$  (blue line) and  $\text{Ni}_2\text{Mn}_{0.75}\text{Cu}_{0.25}\text{Ga}$  (red line) at 80 K. The peaks marked A and B are explained in the text. The arrow in (c) indicates increased XMCD for Ga at the  $L_3$  edge for  $\text{Ni}_2\text{Mn}_{0.75}\text{Cu}_{0.25}\text{Ga}$  as compared with  $\text{Ni}_2\text{MnGa}$ .

to completely fill its  $s$  and  $d$  shells. This can then explain the negligible changes in the Cu XAS.

Comparisons of element-specific magnetic properties between  $\text{Ni}_2\text{MnGa}$  and NMCG at 80 K are shown in Fig. 4. The XMCD signal of NMCG is less than that of  $\text{Ni}_2\text{MnGa}$ , consistent with SQUID magnetometry [Fig. 1(a)]. The Mn-XMCD spectrum for NMCG has a less pronounced multiplet structure than  $\text{Ni}_2\text{MnGa}$  and show less changes between samples than do the Ni spectra. The distinct shoulder A observed in  $\text{Ni}_2\text{MnGa}$  is broadened and feature B is weakened [Fig. 4(a)]. Furthermore, the leading  $L_3$  magnetic circular dichroism peak is shifted to higher energy in NMCG compared to  $\text{Ni}_2\text{MnGa}$ . A localized system should show more multiplet structures in the XAS and XMCD spectra than an itinerant (e.g., metallic) system. The increased itinerancy of the  $3d$  electrons in metallic systems broadens the spectral line shape. Therefore, the smeared multiplets observed in the XAS and XMCD measurements in NMCG indicate that the Ni  $d$  electrons are more delocalized than in  $\text{Ni}_2\text{MnGa}$ . From the evidence of a higher level of hybridization between the Ni  $d$  and Ga  $p$  bands [cf. the Ga-XMCD results in Fig. 4(c)], this indicates that the Ni has a more covalent character with larger band spreading.

#### IV. SUMMARY

The above results show that a complex interplay between electronic, lattice, and magnetic degrees of freedom deter-

mines the decrease (increase) in  $T_C$  ( $T_M$ ) in Cu-substituted  $\text{Ni}_2\text{MnGa}$ . The hybridization and delocalization was found to be affected both by the structural transition as well as by Cu substitution. In particular, we find that, by substituting 25% of Mn by Cu, the ferromagnetic cubic phase is suppressed and a single paramagnetic-cubic to ferromagnetic-tetragonal phase transition takes place at 317 K. This transition is first order in nature indicating that the magnetic transition in NMCG is directly coupled to the structural transition. In general, the NMCG XAS and XMCD spectra were found to have a broader and less-defined multiplet structures than  $\text{Ni}_2\text{MnGa}$  which means that NMCG is relatively a more delocalized system. Thus, the magnetism is no longer confined to Mn alone as is the case for  $\text{Ni}_2\text{MnGa}$  and it is possible that minority spins of Mn would interact with Ni spins to form a band.<sup>15,20</sup> The magnetic interactions are weakened by Cu thereby reducing the overall magnetization and  $T_C$ . We also observe that in spite of the substitution being at the Mn site, more significant spectral changes are evident in the Ni spectra compared to the Mn spectra. Cu substitution results in an enhancement of Ni covalency and therefore a stronger Ni-Ga chemical bond. Since the martensitic transition is related to the formation of Ni  $d$  and Ga  $p$  hybrid states,<sup>17,21</sup> a higher degree of Ni-Ga hybridization in NMCG results in stronger bonding so that more energy is required to trigger the martensitic transition, resulting in an increase in  $T_M$ . Addition of Cu therefore simultaneously increases  $T_M$  at the same time as reducing  $T_C$ , and at 25% Cu substitution  $T_C$  and  $T_M$  coincide near room temperature, giving rise to the giant magnetocaloric effect.

The alloying-induced changes in electronic properties that we observe here clearly influence both the structural and magnetic transitions so that they occur at approximately the same temperature. From our limited set of data it is difficult to isolate the individual influences of the structural and magnetic transitions on the temperature dependence of the NMCG spectra. Future studies of a broader range of compositions and temperatures, coupled with theoretical modeling, may shed more light on the interesting question of how the two transitions merge or coexist to contribute to the magnetocaloric effect.

#### ACKNOWLEDGMENTS

Work at ALS/LBNL was supported by the Director, Office of Science, Office of Basic Energy Sciences, of the U.S. DOE (Contract No. DE-AC02-05CH11231). This work has benefited from use of the Lujan Neutron Scattering Center, funded by the U.S. DOE/BES. LANL is operated by Los Alamos National Security LLC under DOE under Contract No. DE-AC02-06NA25396. Work at UCSD was supported by the U.S. DOE/BES under Contract No. DE-FG01-04ER04-01. Work at SIUC was supported by Research Corporation (Grant No. RA0357) and by the U.S. DOE/BES under Contract No. DE-FG02-06ER46291.

- <sup>1</sup>L. Pareti, M. Solzi, F. Albertini, and A. Paoluzi, *Eur. Phys. J. B* **32**, 303 (2003).
- <sup>2</sup>K. Ullakko, J. K. Huang, C. Kantner, R. C. O'Handley, and V. V. Kokorin, *Appl. Phys. Lett.* **69**, 1966 (1996).
- <sup>3</sup>X. Zhou, W. Li, H. P. Kunkel, and G. Williams, *J. Phys.: Condens. Matter* **16**, L39 (2004).
- <sup>4</sup>C. Biswas, R. Rawat, and S. R. Barman, *Appl. Phys. Lett.* **86**, 202508 (2005).
- <sup>5</sup>M. Khan, I. Dubenko, S. Stadler, and N. Ali, *J. Phys.: Condens. Matter* **16**, 5259 (2004).
- <sup>6</sup>F. Hu, B. Shen, and J. Sun, *Appl. Phys. Lett.* **76**, 3460 (2000).
- <sup>7</sup>J. Marcos, A. Planes, Ll. Mañosa, F. Casanova, X. Batlle, A. Labarta and B. Martínez, *Phys. Rev. B* **66**, 224413 (2002).
- <sup>8</sup>M. Pasquale, C. P. Sasso, L. H. Lewis, L. Giudici, T. Lograsso, and D. Schlögl, *Phys. Rev. B* **72**, 094435 (2005).
- <sup>9</sup>M. Khan, I. Dubenko, S. Stadler, and N. Ali, *J. Appl. Phys.* **97**, 10M304 (2005).
- <sup>10</sup>S. Stadler, M. Khan, J. Mitchell, N. Ali, A. M. Gomes, I. Dubenko, A. Y. Takeuchi, and Alberto P. Guimarães, *Appl. Phys. Lett.* **88**, 192511 (2006).
- <sup>11</sup>B. R. Gautam, I. Dubenko, J. C. Mabon, S. Stadler, and N. Ali, *J. Alloys Compd.* **472**, 35 (2009).
- <sup>12</sup>V. K. Pecharsky and K. A. Gschneidner, Jr., *Phys. Rev. Lett.* **78**, 4494 (1997).
- <sup>13</sup>O. Tegus, E. K. Brück, H. J. Buschow, and F. R. de Boer, *Nature (London)* **415**, 150 (2002).
- <sup>14</sup><http://www.epa.gov>; <http://www.arap.org/index.html>
- <sup>15</sup>J. Kübler, A. R. Williams, and C. B. Sommers, *Phys. Rev. B* **28**, 1745 (1983).
- <sup>16</sup>E. Sasioglu, L. M. Sandratskii, and P. Bruno, *Phys. Rev. B* **77**, 064417 (2008).
- <sup>17</sup>P. A. Bhoje, K. R. Priolkar, and P. R. Sarode, *Phys. Rev. B* **74**, 224425 (2006).
- <sup>18</sup>P. J. Brown, J. Crangle, T. Kanomata, M. Matsumoto, K.-U. Neumann, B. Ouladdiaf, and K. R. A. Ziebeck, *J. Phys.: Condens. Matter* **14**, 10159 (2002).
- <sup>19</sup>A. Ayuela, J. Enkovaara, and R. M. Nieminen, *J. Phys.: Condens. Matter* **14**, 5325 (2002).
- <sup>20</sup>S. R. Barman, S. Banik, and A. Chakrabarti, *Phys. Rev. B* **72**, 184410 (2005).
- <sup>21</sup>A. T. Zayak, P. Entel, K. M. Rabe, W. A. Adeagbo, and M. Acet, *Phys. Rev. B* **72**, 054113 (2005).
- <sup>22</sup>N. A. de Oliveira and P. J. von Ranke, *Phys. Rev. B* **77**, 214439 (2008).
- <sup>23</sup>G. J. Liu, J. R. Sun, J. Shen, B. Gao, H. W. Zhang, F. X. Hu, and B. G. Shen, *Appl. Phys. Lett.* **90**, 032507 (2007).
- <sup>24</sup>G. Jakob, T. Eichhorn, M. Kallmayer, and H. J. Elmers, *Phys. Rev. B* **76**, 174407 (2007).
- <sup>25</sup>A. Kimura, S. Suga, T. Shishidou, S. Imada, T. Muro, S. Y. Park, T. Miyahara, T. Kaneko, and T. Kanomata, *Phys. Rev. B* **56**, 6021 (1997).
- <sup>26</sup>M. Kallmayer, H. J. Elmers, B. Balke, S. Wurmehl, F. Emmertling, G. H. Fecher, and C. Felser, *J. Phys. D* **39**, 786 (2006).
- <sup>27</sup>W. H. Wang, M. Przybylski, W. Kuch, L. I. Chelaru, J. Wang, Y. F. Lu, J. Barthel, H. L. Meyerheim, and J. Kirschner, *Phys. Rev. B* **71**, 144416 (2005).
- <sup>28</sup>A. Chakrabarti, C. Biswas, S. Banik, R. S. Dhaka, A. K. Shukla, and S. R. Barman, *Phys. Rev. B* **72**, 073103 (2005).
- <sup>29</sup>P. J. Brown, A. Y. Bargawi, J. Crangle, K.-U. Neumann, and K. R. A. Ziebeck, *J. Phys.: Condens. Matter* **11**, 4715 (1999).
- <sup>30</sup>S. M. Butorin, J.-H. Guo, M. Magnuson, P. Kuiper, and J. Nordgren, *Phys. Rev. B* **54**, 4405 (1996).
- <sup>31</sup>S. Imada, A. Yamasaki, T. Kanomata, T. Muro, A. Sekiyama, and S. Suga, *J. Magn. Magn. Mater.* **310**, 1857 (2007).
- <sup>32</sup>D. Haskel, Y. B. Lee, B. N. Harmon, Z. Islam, J. C. Lang, G. Srajer, Ya. Mudryk, K. A. Gschneidner, Jr., and V. K. Pecharsky, *Phys. Rev. Lett.* **98**, 247205 (2007).